Effective wave dispersion and attenuation in three-periodic thin poroelastic layers saturated by two-phase fluids.

*Juan E. Santos * School of Earth Sciences and Engineering, Hohai University, Universidad de Buenos Aires, Facultad de Ingeniería, Instituto del Gas y del Petróleo, Department of Mathematics, Purdue University, José M. Carcione, Istituto Nazionale di Oceanografia e di Geofisica Sperimentale (OGS), Borgo Grotta Gigante 42c, 34010 Sgonico, Trieste, Italy, Gabriela B. Savioli, Universidad de Buenos Aires, Facultad de Ingeniería, Instituto del Gas y del Petróleo and Patricia M. Gauzellino, Facultad de Ciencias Astronómicas y Geofísicas, Universidad Nacional de La Plata*

SUMMARY

Wave induced fluid flow (WIFF) in fluid-saturated poroelastic media occurs due to conversion of fast to slow diffusion P-waves at mesoscopic scales, which are much larger than the average pore size and much smaller than the traveling fast P-wave wavelengths. In this works we show than in hydrocarbon reservoirs, where the pore space is saturated by two-phase fluids, capillary pressure and interference betweeen the two fluid phases as they flow induce additional velocity attenuation and dispersion of seismic waves. We present a Finite Element (FE) procedure to determine the phase velocities and dissipation factors in a three-periodic fine layered poroelastic medium saturated by two-phase fluids. The results are first compared with those of single-phase effective fluids and then cases of patchy saturation are analyzed. The results show that residual saturations and wettability influence the effective P-wave phase velocities and dissipation factors.

INTRODUCTION

Wave induced fluid flow (WIFF) occures by mode conversion at mesoscopic scale heterogeneities in the petrophysical and fluid properties. WIFF is responsible for the high levels of attenuation of seismic waves observed in rocks with partial saturation. Wave propagation in poroelastic materials saturated by single-phase fluids was presented by Biot in seminal papers (Biot, 1956, 1962), where is predicted the existence of two P-waves, one fast and slow, and one shear wave. To analyze the effects of capillary pressure and fluid-flow interferences as they flow within the pore space, we use an extension of Biot's theory presented in several papers **????**.

This extension of Biot's theory predicts the existence of three compressional waves (P1, fast, P2 and P3, slow) and one shear wave. Capillary pressure and relative flow between the two fluid phases induce additional energy losses that can not be represented using effective single-phase fluids. The model for capillary pressure and relative permeabilities used in this work is that of **?**, where is possible that simultaneous flow of both phases occurs along what must be very tortuous funicular paths (funicular regime).

White and coauthors **?** were the first to study the WIFF mechanism. They considered the seismic response of plane thin layers alternately saturated with gas and water. Later, **?** implicitly extended the results for many layers and **?** found the explicit analytical solution for three layers.

In this work we analyze the mesoscopic effect on three-periodic sequences of thin layers much smaller then the average wavelengths. Hence, Biot's equations are be solved in the diffusive range of frequencies, as presented in Santos et al. (2009). In this approach we apply compressibility tests to a representative sample of the layered material and measure the resulting stress and strains, which quotient yields the desire P-wave modulus. First the results are compared with those of single-phase fluids. Then several cases of three-periodic samples with patchy gas-oil, gas-brine and brine-oil are presented.

THE MODEL EQUATIONS

In the three-periodic poroelastic sample saturated by a two-phase fluids we have a solid phase and wetting and non-wetting phases, indicated by the subindexes or superindexes s, w, n. Let S_w, S_n. Let S_w, S_n denote the wetting and non-wetting saturations, with S_{rw} and S_{rn} being the associated residual saturations. It is assumed that the two-phase fluid completely saturates the pore space, so that $S_w + S_n = 1$, with immobile wetting fluid in $[0, S_{rw}]$ and immobile non-wetting fluid in $[0, S_{rn}]$, and $S_{rw} > 0$.

Furthermore, we assume a funicular regime of flow, so that each fluid phase occupies continuous paths, where both fluids simultaneously flow. Then, we have

$$S_{rw} < S_w < 1 - S_{ro}, \quad S_{ro} < S_o < 1 - S_{rw}. \tag{1}$$

The diffusion equations for a poroelastic medium saturated by a two-phase fluid are **??**:

$$\nabla \cdot \tau(\mathbf{u}) = 0, \tag{2}$$

$$i\omega\, d_n\, \mathbf{u}^n - i\omega\, d_{nw}\, \mathbf{u}^w + \nabla \mathscr{T}_n(\mathbf{u}) = 0, \tag{3}$$

$$i\omega\, d_w\, \mathbf{u}^w - i\omega\, d_{nw}\, \mathbf{u}^n + \nabla \mathscr{T}_w(\mathbf{u}) = 0. \tag{4}$$

The constitutive equations, with ε_{ij} denoting the strain tensor, are

$$\tau_{ij}(\mathbf{u}) = 2\mu\, \varepsilon_{ij} + \delta_{ij}(\lambda_u\, e^s - F_1\, \xi^n - F_2\, \xi^w), \tag{5}$$

$$\mathscr{T}_n(\mathbf{u}) = (S_n + \beta) P_n - \beta P_w = -F_1\, e^s + N_1\, \xi^n + N_3\, \xi^w \tag{6}$$

$$\mathscr{T}_w(\mathbf{u}) = S_w\, P_w = -F_2\, e^s + N_3\, \xi^n + N_2\, \xi^w. \tag{7}$$

The coefficients in the constitutive equations 5 - 7, defining the generalized forces τ_{ij}, $\mathscr{T}_n$ and $\mathscr{T}_w$, are computed as indicated in (**??**).

THE FE HARMONIC EXPERIMENTS

Equations (2)-(4) will be solved for representative sample consisting of a three-periodic sequence of fine layered square sample $\Omega = (0,L)^2$ with boundary Γ in the (x,z)-plane. The complex P modulus characterizing the long-wave behavior to our sample Ω is determined by applying comppressibility time-harmonic tests in the normal direction to the layering. This test is associated with a boundary value problem for equations (2)-(4) that is solved using the FE method. For detailed formulations on the definition of harmonic tests and their FE computer implementation for the case poroelastic materials we refer to Santos and Gauzellino (2017).

NUMERICAL RESULTS

We consider a square sample and six periods, each consisting of three 20 cm layers, referred to as layers1, 2 and 3, saturated by a two-phase fluid. The sample is discretized using a 90×90 uniform mesh. The relative permeability and capillary pressure functions are defined as (**??**):

$$K_{rn}(S_n) = (1-(1-S_n)/(1-S_{rn}))^2, \tag{8}$$

$$K_{rw}(S_n) = ([1-S_n-S_{rw}]/(1-S_{rw}))^2, \tag{9}$$

$$P_{ca}(S_n) = A\left(1/(S_n+S_{rw}-1)^2 - S_{rn}^2/[S_n(1-S_{rn}-S_{rw})]^2\right), \tag{10}$$

where A is the capillary pressure amplitude. In all examples $A = 30$ kPa, $S_{rn} = 0$ and the matrix and fluid properties are given in Tables 1 and 2, respectively.

Table 1. Properties of the sandstone

Grain bulk modulus, K_s	33.4 GPa
density, ρ_s	2650 kg/m^3
Dry-matrix bulk modulus, K_m	1.3 GPa
shear modulus, μ	1.4 GPa
porosity, ϕ	0.3
permeability, κ	10^{-12} m^2

Table 2. Properties of the saturant fluids

Brine bulk modulus, K_w	2.2 GPa
density, ρ_w	975 kg/cm^3
viscosity, η_w	0.001 Pa $\cdot$ s
Oil bulk modulus, K_o	2 GPa
density, ρ_o	870 kg/cm^3
viscosity, η_o	0.3 Pa $\cdot$ s
Gas bulk modulus, K_g	0.0044515 GPa
density, ρ_g	42.316 kg/m^3
viscosity, η_g	1.1186×10^{-5} Pa $\cdot$ s

Comparison with effective single-phase fluids

We consider the first experiment, (Experiment 1 in the text and Figures), where brine is the wetting phase in the three layers, $S_{rw} = 1\%$ and on each three-periodic layering layer 1 has gas-brine saturation, 0.12 % gas, layer 2: gas-brine saturation, 98 % gas and layer 3: oil-brine saturation, 98 % oil. The theory of **?** for layered three-periodic poroelastic media holds for single-phase fluids. Thus we compare our FE results with those of an effective single-phase fluid using a Reuss average of the fluid bulk modulus and an arithmetic average of the densities and viscosities of each fluid phase . The corresponding results in the next figures are labeled *single-phase model*. For single-phase fluids, the approximate location of the relaxation peak is (**?**)

$$f_r = \frac{8\kappa M E_m}{\pi \eta L^2 E_c} \tag{11}$$

where $M = \left[(\alpha-\phi)/K_s + \phi/K_f^*\right]^{-1}$, $\alpha = 1-K_m/K_s$, $E_m = K_m + 4/3\mu$, $E_c = K_c + 4\mu/3$, $K_c = K_m + \alpha^2 M$, and L is the spatial period. Hence, as viscosity increases or permeability decreases, the attenuation peak moves to lower frequencies.

Figures1 and 2 show the effective P-wave phase velocities and dissipation factors (1000/Q) as a function of frequency for Experiment 1. P-wave velocities are quite close for both models, and two attenuation peaks are seen in Figure 2, as predicted by the theory for single-phase fluids in **?**. The higher peak for the two-phase model is shifted to higher frequencies as compared with that of the single-phase model. According to equation 11, the lower and higher frequency attenuation peaks correspond to the presence of oil and gas, respectively.

patchy saturation

Fractal variations of gas, oil or brine saturation (patchy saturation) are obtained by using the von Karman autocorrelation function with 2D wave number-domain power spectrum given by (Frankel and Clayton, 1986; **?**; **?**)

$$P(k_x,k_z) = (1+k^2\mathrm{a}^2)^{-(H+N_e/2)} \tag{12}$$

where $k = \sqrt{k_x^2+k_z^2}$ is the wave-number, N_e is the Euclidean dimension, a is the correlation length and H is the Hurst exponent, $0 < H < 1$). Equation 12 defines a fractal process of dimension $D = N_e + 1 - H$ at scales smaller than a. In the following examples N_e = 2, D = 2.2 and a approximately 0.5 % of the domain size.

The next example, referred to as Experiment 2,

considers brine as the wetting phase in the three layers, with $S_{rw} = 10\%$ and layer 1 with gas-brine saturation, 0.12 % gas, layer 2 with patchy gas-brine saturation, overall gas saturation 10 % or 30 % and layer 3 with oil-brine saturation, 89 % oil.

Figures 3 and 4 display the phase velocity and dissipation factor for Experiment 2 and overall patchy gas-brine saturations of 10 % and 30 % in layer 2. Figure 3 shows higher velocities for non-patchy than for patchy saturation in layer 2 (about 17 % higher) and quite similar velocities for both values of the overall gas saturation, except at higher frequencies, with values for 30% and 10 % patchy saturation below and above that of non-patchy saturation, respectively. Figure 4 shows two attenuation peaks for both overall saturations, which at lower frequencies are associated with the oil phase and at higher frequencies correspond to the gas phase. The peaks for non-patchy saturation are close each other, and located at lower

frequencies compared to those of Experiment 1 in Figure 2. the difference between these two curves is due to the different values of saturations and residual oil and gas saturations.

Figure 5 display plot of the fluid pressure at 20 Hz for 10 % overall gas saturation in Layer 2 fo Experiment 2. The fluid pressure is computed as $\mathscr{T} = \mathscr{T}_n + \mathscr{T}_w$, with $\mathscr{T}_n, \mathscr{T}_w$ defined in equations 6-7. The gradients of fluid pressure illustrate the mesoscopic loss mechanism.

Finally, Experiment 3, with $S_{rw} = 10\%$ considers the case in which layer 1 has gas-brine saturation, 0.12 % gas, brine is the wetting phase, layer 2 has patchy gas-oil saturation, oil is the wetting phase and layer 3 has patchy brine-oil saturation, with oil being the wetting phase. Overall gas/brine saturations 10 % and 40 %.

Figure 6 exhibit dissipation factors for the two-phase and single-phase models for Case 6. It can be observed two attenuation peaks for the two-phase model, much higher at low frequencies for the lowest overall patchy saturation (an expected result), while the single-phase model exhibits a single peak. Furthermore, the attenuation peak is wider as compared with the previous cases. These differences in attenuation are associated with the fact that in the two-phase model oil is the wetting phase in Layers 2 and 3. This assumption generates flow interactions between the two fluids via the relative permeability functions in a way that induces a second peak, an effect that is not predicted when using single-phase fluids.

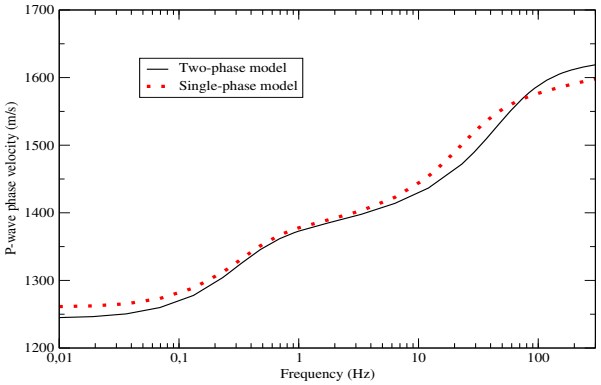

Figure 1: P-wave phase velocity as a function of frequency for the two-phase and single-phase fluid models. Case 1

CONCLUSIONS

It is observed that the presence of capillary forces and the relative flow between the two fluids induce noticeable changes in phase velocity and attenuation of the P-wave when compared with single-phase fluids. Besides, the velocities predicted for non-patchy saturation are generally higher than those obtained for patchy saturation.

One additional and important factor in reservoir rocks saturated by two-phase fluids is wettability, i.e., the role of each fluid as wetting or non-wetting phase. In the numerical simulations, interchanging the roles of the wetting and non-wetting

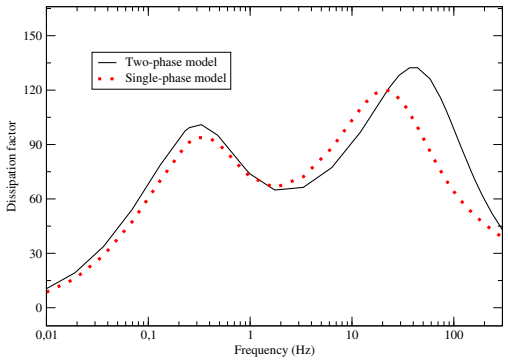

Figure 2: P-wave dissipation factor as a function of frequency for the two-phase and single-phase fluid models. Case 1

Figure 3: P-wave phase velocity as a function of frequency for the two-phase model for Cases 1 and 3. Overall gas saturations in Layer 2 are 10 % and 30 %

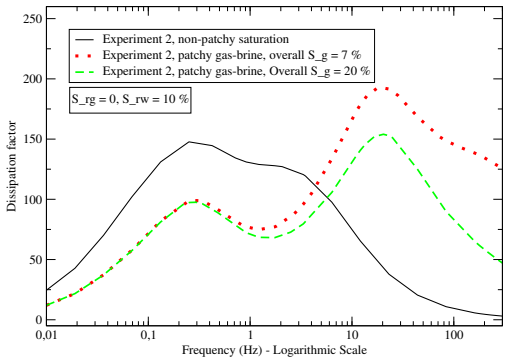

Figure 4: P-wave dissipation factor as a function of frequency for the two-phase model for Cases 1 and 3. Overall gas saturations in Layer 2 are 10 % and 30 %

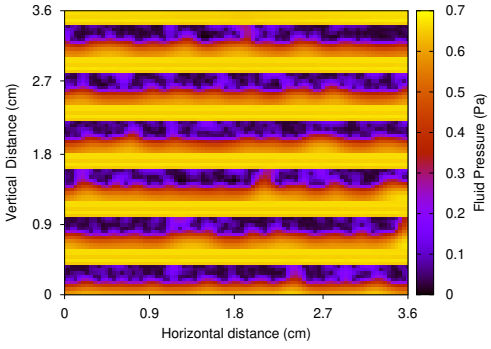

Figure 5: Fluid pressure at 20 Hz for Case 3. Overall gas saturation in Layer 2 is 10 %.

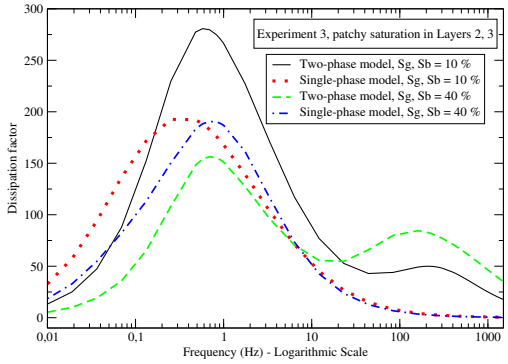

Figure 6: . P-wave dissipation factor as a function of frequency for the two-phase and single-phase models for case 6. Overall gas/brine saturations are 10 % and 40 %.

fluids, either two or one attenuation peaks are obtained, a result that cannot be predicted by the Biot theory, valid for single-phase fluids. In summary, the simulations predict dispersion and attenuation effects in hydrocarbon reservoir rocks that cannot be described if single-phase fluids are used.

ACKNOWLEDGMENTS

This work was partially funded by ANPCyT, Argentina (PICT 2015 1909) and Universidad de Buenos Aires (UBACyT 20020160100088BA)

REFERENCES

Biot, M. A., 1956, Theory of deformation of a porous viscoelastic anisotropic solid: J. Appl. Phys., **27**, 459–467.

———, 1962, Mechanics of deformation and acoustic propagation in porous media: J. Appl. Phys., **33**, 1482–1498.

Frankel, A. and R. W. Clayton, 1986, Finite difference simulation of seismic wave scattering: implications for the propagation of short period seismic waves in the crust and models of crustal heterogeneity: Journal of Geophysical Research, **91**, 6465–6489.

Santos, J. E. and P. M. Gauzellino, 2017, Numerical simulation in applied geophysics: Birkhauser, Lecture Notes in Geosystems Mathematics and Computing.

Santos, J. E., J. G. Rubino, and C. L. Ravazzoli, 2009, A numerical upscaling procedure to estimate effective plane wave and shear moduli in heterogeneous fluid-saturated poroelastic media: Comput. Methods Appl. Mech. Engrg, **198**, 2067–2077.